Preparation of Functionalized Superparamagnetic Fe₃O₄@Dopamine@Metal Ions (Cu⁺,Ru²⁺) Nanocomposites and its Catalytic Applications

Renuka Singh[1], Shukla Majhi[1], Keshav Sharma[1], Mohd. Ali[2], Chandra Shekhar Pati Tripathi[*2], and Debanjan Guin[*1]

[1]Department of Chemistry, Institute of Science, Banaras Hindu University Varanasi- 221005, Uttar Pradesh, India.
Email: debanjan.chem@bhu.ac.in
[2]Department of Physics, Institute of Science, Banaras Hindu University Varanasi- 221005, Uttar Pradesh, India.
Email: tripathi.csp@bhu.ac.in

Abstract

In this work, we present a simple method for the synthesis of metal ions stabilized on dopamine modified iron oxide nanoparticles (Fe_3O_4@DA@M^{x+}) and their catalytic applications in important organic transformation reactions. Two different metal ions (Cu^{+1} and Ru^{2+}) are studied in this work. It is observed that both synthesized Fe_3O_4@DA@Cu$^+$ and Fe_3O_4@DA@Ru^{2+} can effortlessly be separated from the reaction medium by positioning an external magnetic field. Dopamine, which is used as an anchor between Fe_3O_4 and metal ions, increases the solubility of catalyst in reaction medium and prevents leaching of metal ions from the catalyst surface. Here Fe_3O_4@DA@Cu$^+$ is used in the synthesis of 1,2,3-triazole derivatives via azide-alkyne cycloaddition reactions and Fe_3O_4@DA@Ru^{2+} is used for transfer hydrogenation reaction of various aryl ketones. The Fe_3O_4@DA@M^{x+} nanocomposite is characterized via powder X-ray diffraction (XRD), X-ray photoelectron spectroscopy (XPS), scanning electron microscopy (SEM), transmission electron microscopy (TEM), Fourier transform infrared spectroscopy (FTIR), atomic absorption spectroscopy (AAS), thermogravimetric analysis (TGA) and vibrating-sample magnetometer (VSM). The Fe_3O_4@DA@M^{x+} catalytic systems can be reused in the reaction mixture up to five times without significant loss in their catalytic activity.

Graphical Abstract
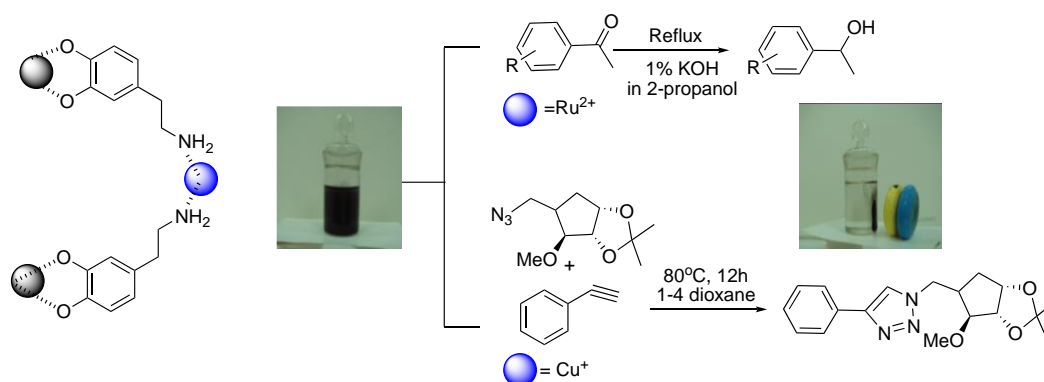
1 Introduction

The stabilization of metal ion catalysts on inorganic supports for their application in important organic transformation reactions has made remarkable progress in the recent years.[1-5] In this context, superparamagnetic nanoparticles as a catalyst support have gained significant attention due to their relatively easy synthesis procedure, high surface activity, good stability, and efficient recovery from the reaction medium.[6, 7]The use of magnetic nanoparticles provide the advantage of effortless separation of the catalyst from the reaction medium just by applying a simple external magnetic field. However, the leaching of metal ion from the support surface hampers the efficiency and reusability of these catalysts. To overcome this issue, the concept of introducing a linker between catalyst and solid support was presented by various research groups. This has helped in improving the long-term stability as well as the dispersity of the catalyst in reaction medium to obtain better catalytic efficiency[1, 8-13].

The application of copper as a homogeneous catalyst has many complexities such as extremely difficult separation method of the catalyst, low recyclability, high cytotoxicity and other environmental related concerns[14]. The increasingly strict regulations in the industrial

application of the catalyst demands the removal of even trace amounts of catalyst from the final product. Even with the extensive methods, the elimination of trace amounts of catalyst from the product is a challenge. Cu^{+1} ions are known to be best catalyst for the synthesis of 1,2,3-Triazole derivatives which is commonly known as 'click 1,2,3 cycloaddition' reaction[15]. 1,2,3-Triazole derivatives are an extremely important class of organic compounds for pharmaceutical applications. They also exhibit a broad range of biological, antiepileptic, anti-allergic, and anti-HIV properties. 1,2,3-Triazole derivatives are prepared through Huisgen dipolar cycloaddition of organic azides and alkynes[16-18]. However, the reaction has an extremely slow rate, produces a mixture of regioisomers and has very low yield even at high temperatures (80–120ºC for 12–24 h). The pioneering work on Cu-catalyzed azide–alkyne cycloaddition (CuAAC) reactions in 2002 led to a major improvement in both the rate and regioselectivity of the reaction[19, 20]. It still continues to attract the interests of researchers. The CuAAC reaction satisfies the criteria of click chemistry and has been extensively applied to chemical synthesis of macromolecules, and functionalization of biomolecules. The exceptional stability of azide and terminal alkynes also make them a suitable candidate for application as starting material in reactions pertaining to biotechnology and materials science[18, 21]. The regioselectivity, increased reactivity of unactivated alkynes, and very high yields even at low concentrations in aqueous media makes CuAAC reaction advantageous over the thermal version.[22] An extremely easy and efficient method for the preparation of heterogeneous Cu catalytic systems based on copper is its immobilization on solid supports. There are plenty of literature available where different solid support systems are used to immobilize copper ions. For the immobilization of copper, various support systems such as activated polymers [23], zeolites [24], graphene [25, 26], carbon

nanotubes[27], silica[28] and iron oxide (Fe_3O_4) nanoparticles[3] others[29-31] have been used so far.

Hydrogenation reaction of aromatic ketones and unsaturated compounds is another class of most fundamental organic transformation reaction in organic synthesis. Its industrial applications ranges from fine chemicals to pharmaceuticals synthesis[32-34]. Two different paths are followed for hydrogenation reaction. One is direct hydrogenation which involves with a pressure of H_2 gas pressure and another is transfer hydrogenation without using H_2 gas pressure. Transfer hydrogenation reactions are smart alternative to direct hydrogenation. It has become the focus of recent research in hydrogenation science as it neither requires any hazardous pressurized H_2 gas nor elaborate experimental setups [35]. Au, Fe, Ru, Rh, Ir ions are commonly used as catalyst for transfer hydrogenation reactions and among all metal ions Ru ions are extensively used as for transfer hydrogenation reaction of aromatic aldehydes and ketones [36-39]. To stabilize Ru ions different types of catalytic support like zeolite, nanoparticles, graphene oxide, carbon, ionic liquids, polymers are used extensively for transfer hydrogenation reactions [40-44].

In this paper, we present the preparation and characterization of heterogeneous metal ions (Cu^{+1} and Ru^{2+}) supported on dopamine (DA) modified Fe_3O_4 nanoparticles. The amine group of dopamine stabilizes the copper/ ruthenium ions and reduces the leaching of Cu^+/Ru^{2+} ions from catalyst support. It also enhances the solubility of the catalyst in the organic solvent. The Fe_3O_4@DA@Cu^+ catalyst promotes the Huisgen 1, 3-dipolar cycloaddition of organic azides and terminal alkynes. It is also found efficient in the reaction between organic halides and terminal alkynes in presence of sodium azide. The Fe_3O_4@DA@Ru^{2+} catalyst efficiently reduce number of aromatic ketone derivatives to their respective alcohol derivatives. Both the prepared catalysts

are easily separable by the application of an external magnet at the end of the reaction. The recovered catalyst can be reused without loss of catalytic activity or leaching of any metal species.

2 Experimental

Characterizations

Fourier transform infrared (FTIR) spectra were recorded on Bruker Alpha T spectrophotometer. X-ray diffraction (XRD) patterns were obtained by a Rigaku Miniflex 600 desktop X-Ray diffractometer with Cu Kα radiation in 2θ range of 5-80Å. Scanning electron microscopy (SEM) images were taken on ZEISS EVO 18 SEM. Nitrogen adsorption and desorption isotherms were obtained with an Autosorb-iQ-MP-XR (Quantachrome, Florida, USA). X-ray photoelectron spectroscopic studies were carried out using a KRATOS AXIS 165 X-ray Photoelectron Spectrometer. Thermogravimetric analysis (TGA) was performed at heating rate of $10^{o}C$ under nitrogen atmosphere using Perkin-Elmer STA 6000 instrument. Atomic absorption spectroscopy (AAS) measurement was carried out using a PerkinElmer (Model-AAnalyst-700) spectrometer. Prior to analysis, the sample was digested in aqua regia. Transmission electron microscopy (TEM) experiments were carried out by a Tecnai G2 20 TWIN electron microscope. Nuclear magnetic resonance (NMR) spectra were recorded on Bruker DRX300 spectrometer using $CDCl_3$ as solvent and tetramethylsilane (TMS) as internal standard. The magnetic properties of samples were measured with a Vibrating Sample Magnetometer (VSM)-LAKESHORE (Model: 7404).

Synthesis of Cu (I)/ Ru (II) on amine terminated Fe_3O_4 nanoparticles

The synthesis of $Fe_3O_4@DA@M^{x+}$ (M^{x+} = Cu^+/Ru^{2+}) catalytic system is shown in **Scheme 1**. It consists of two major steps. In the first step, Fe_3O_4 nanoparticles have been synthesized by coprecipitation of $FeCl_2$ and $FeCl_3$ in presence of dopamine hydrochloride in aqueous medium. In brief, $FeCl_2$ and $FeCl_3$ (1:2 molar ratio) were dissolved in doubly distilled water acidified with HCl during continuous stirring at ambient temperature and pressure to obtain a clear solution. Into which 0.189 g (1mmol) of dopamine hydrochloride was added. Hydrazine monohydrate was added dropwise to adjust the pH of the solution to almost 10. The reaction mixture was stirred further for a period of 2 h. The black precipitate was collected, filtered and repeatedly washed with distilled water. The product dopamine capped Fe_3O_4 nanoparticles was subsequently dried in vacuum for 2 h at room temperature.

In the second step, 0.049 g (0.25 mmol) of cupric acetate monohydrate was dissolved in 50 mL of distilled water and mixed with 50 mL of aqueous solution of dopamine capped Fe_3O_4 containing 0.5 g of dopamine capped Fe_3O_4 NPs. The pH of the solution was adjusted to 10 and stirred at 25°C for 2 h. After several washings with water to remove impurities followed by magnetic separation, a highly pure $Fe_3O_4@DA@Cu^+$ catalyst system was obtained.

By similar method 0.5 g of as synthesized dopamine capped Fe_3O_4 nanoparticles were taken in 50 mL deionized water and 0.48 mmol (0.1 g) of $RuCl_3$ was introduced into the mixture. The reaction mixture was sonicated for 30 min to get highly dispersed solution. The reaction mixture was then refluxed for 2 h in N_2 atmosphere. The mixture was then cooled to room temperature. Excess acetone was added to the mixture to precipitate the catalyst. The precipitate was washed several times with water and finally separated by applying external magnetic field and the powder was subsequently dried in vacuum to get $Fe_3O_4@DA@Ru^{2+}$ catalytic system.

Scheme 1.
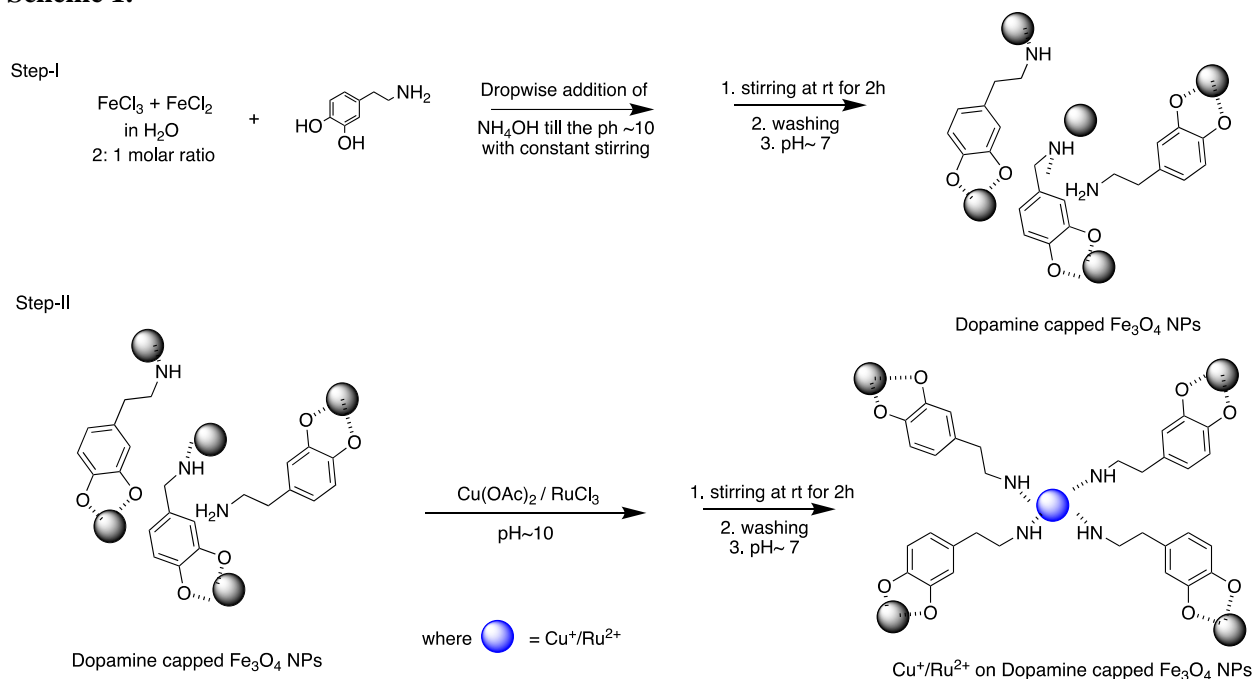
Scheme 1: Synthesis procedure of $Fe_3O_4@DA@M^{x+}$ ($M^{x+} = Cu^+/Ru^{2+}$) catalyst system

3 Results and Discussion

The $Fe_3O_4@DA@M^{x+}$ catalytic system was characterized using various experimental techniques such as XRD, XPS, SEM, TEM, BET, TGA, AAS, FT-IR, and VSM.

The powder X-ray diffraction patterns of the dopamine capped Fe_3O_4 catalyst system was measured and are shown in **Fig. 1** which shows the crystalline nature of the nanocatalyst. The pattern observed during the measurement was compared with the standard Fe_3O_4 pattern (JCPDS (The Joint Committee on Powder Diffraction Standards) card no. 19-0629). Eight typical peaks were observed at 18.4^o, 30.1^o, 35.4^o, 43.2^o, 53.4^o, 57.2^o, 62.5^o, and 74.3^o, which are due to the diffraction of the (111), (220), (311), (400), (422), (511), (440), and (533) lattice planes of Fe_3O_4, respectively.
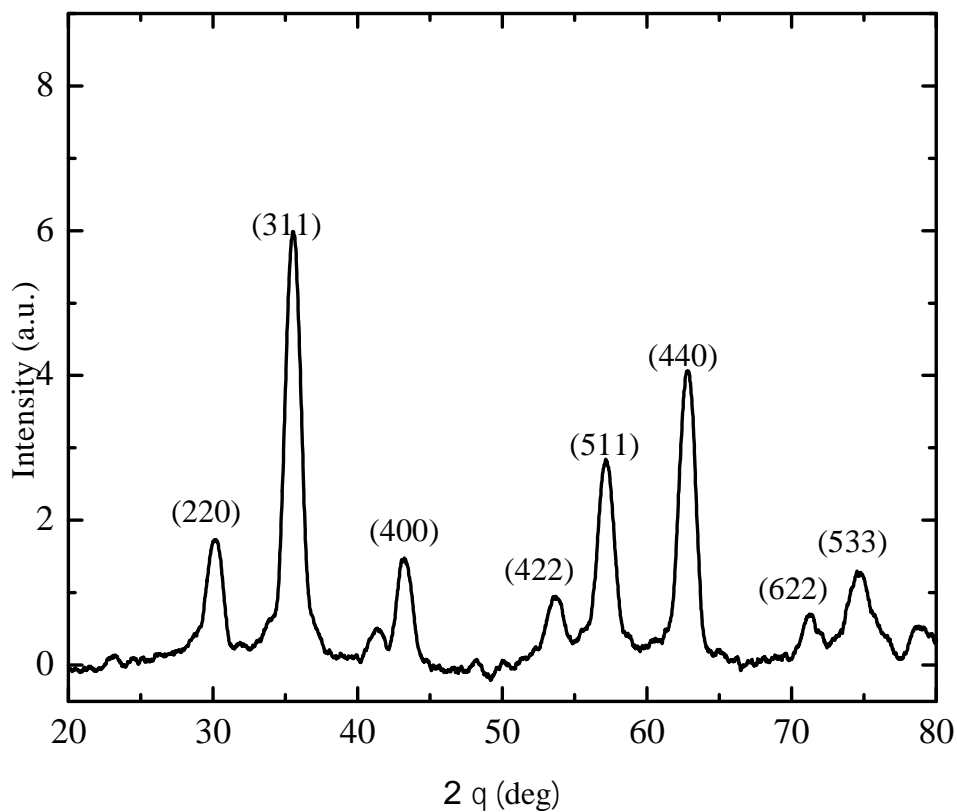
Fig. 1 XRD patterns of dopamine capped Fe_3O_4 NPs

The FTIR spectra of $Fe_3O_4@DA$ is shown in Fig.2. The broad peak at 3390 cm^{-1} has been
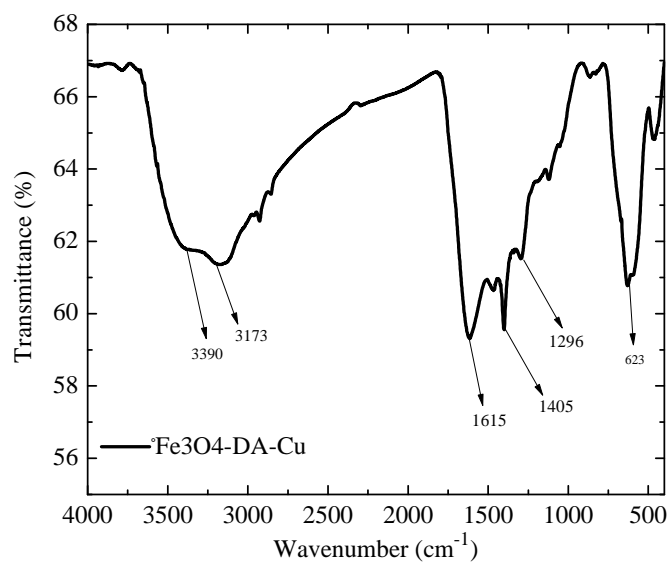

Fig. 2 FTIR spectra of $Fe_3O_4@DA$ NPs.

assigned to the surface absorbed water, NH stretching vibration and OH stretching vibrations. The peak at ~1615cm^{-1} can be assigned to N-H bending vibrations. The absorption bands in the FTIR spectrum of Fe_3O_4-DA-Cu^+ at ~1405 cm^{-1} and ~1296 cm^{-1} are assigned as ν (C=C) and ν (C–N) of the dopamine coating. The peak at ~600 cm^{-1} confirms the presence of iron oxide nanoparticles.

The scanning electron microscopy (SEM) image of Fe_3O_4@DA is shown in **Fig. 3.** The SEM image reveals the morphology of the catalyst surface, which is rough due to the presence of magnetic nanoparticles.
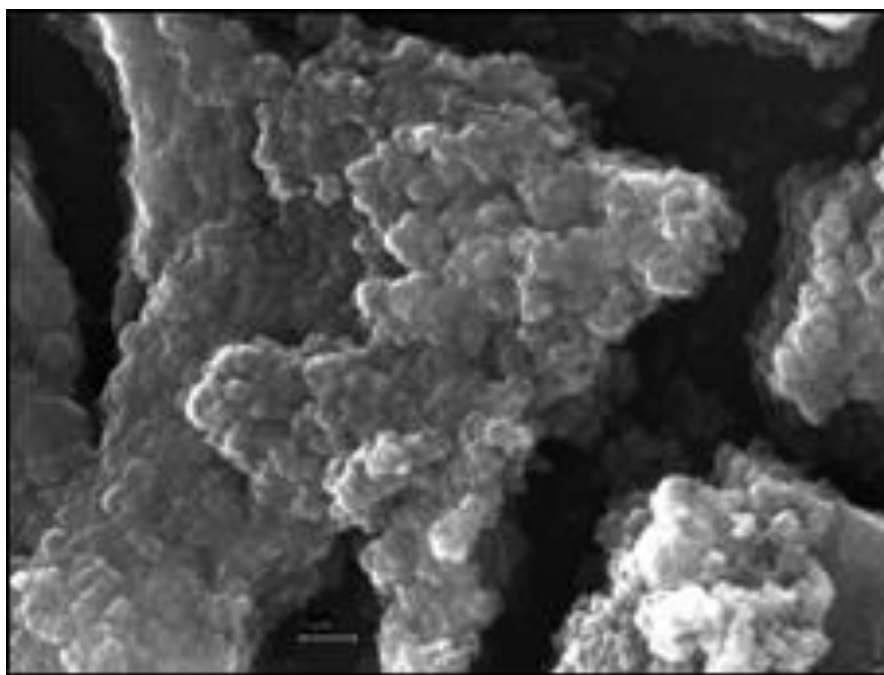
Fig. 3 SEM images of Fe_3O_4@DA

Thermogravimetric analysis (TGA) analysis of Fe_3O_4@DAwas performed in the range of 25 to 600 ^{o}C to determine the loading of organic groups coated onto the surface of the magnetite. SI Fig 1 shows the TGA of Fe_3O_4@DA. In all the samples, the weight loss within 100–200 ^{o}C is due to the physically adsorbed water molecules and hydroxyl groups at the surface of the Fe_3O_4.

Fe$_3$O$_4$@DA shows a 15% weight loss at 250–600 ºC corresponding to the thermal decomposition of the dopamine groups on the surface of Fe$_3$O$_4$.

The TEM image of the freshly prepared Fe$_3$O$_4$@DA@Cu$^+$ catalyst is shown in **Fig. 4 (a)**. It is observed that the synthesized particles are about 45-50 nm in size. The TEM image of the catalyst after five repeated reactions **(Fig. 4 (b))** shows some agglomeration but overall no change in the morphology of the particle was observed.
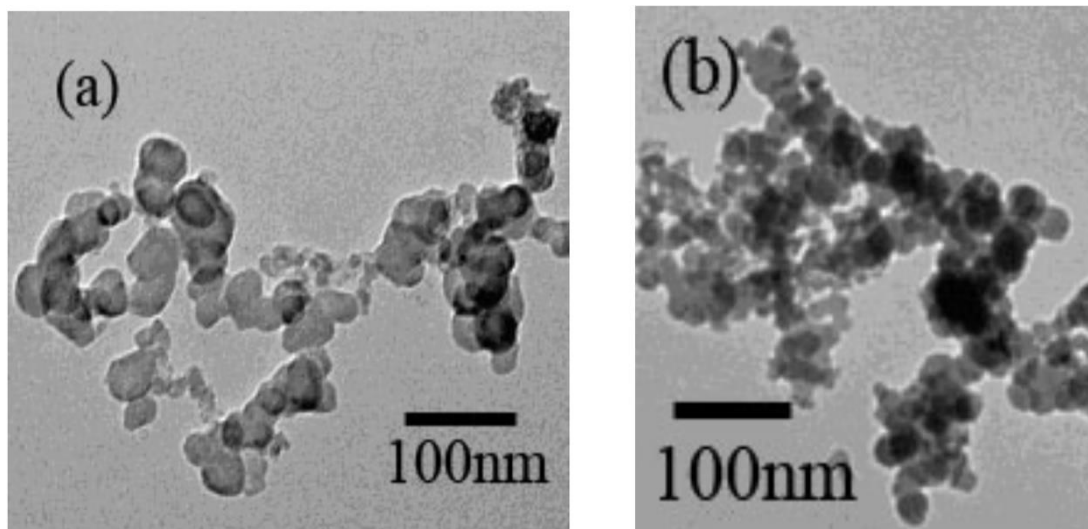

Fig. 4 TEM images of (a) Fe$_3$O$_4$@DA@Cu$^+$ and (b) recovered Fe$_3$O$_4$@DA@Cu$^+$ catalyst after the fifth run.

TEM images of Fe$_3$O$_4$@DA@Ru^{2+} catalytic system also recorded. Fig. 5 (a) shows the TEM micrographs of the Fe$_3$O$_4$@DA@Ru^{2+} catalyst before reaction. It is observed that the synthesized particles are nearly spherical, about 45-50 nm in size. Fig. 5. (b) shows the TEM micrograph of catalyst after 5 repeated reactions, which shows agglomerated particles with an average size around 50 nm.
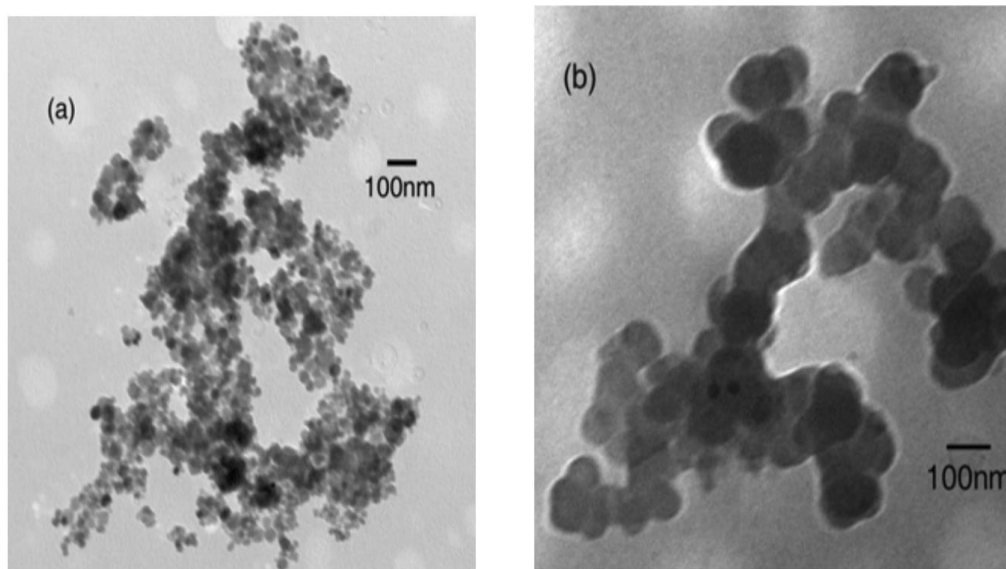
Fig. 5(a) and (b) TEM micrographs of the $Fe_3O_4@DA@Ru^{2+}$ catalyst (a) before (b) after 5 repeated cycles.

X-ray photoelectron spectroscopy studies were carried out to establish the oxidation state of Cu and Ru present in their respective catalyst systems. SI Fig. 2(a) shows the XPS spectrum of Cu. The Cu $2p_{3/2}$ binding energy spectrum is fitted using the nonlinear least-square fit program using Gaussian equation. The spectrum consists of a single peak at 931.3 eV with an FWHM of 3.2eV. This peak is attributed to the Cu in +1 oxidation state, which agrees with the reported data. The oxidation state +1 of Cu is known to be most active for "Click Reactions". SI Fig. 2 (b) is the Ru $3p_{3/2}$ binding energy spectrum fitted using the nonlinear least-square fit program using Gaussian-Lorentzian equation. The spectrum consists of a single peak at 463.05eV with an FWHM of 3.725. This peak is attributed to the Ru in 2+ oxidation state that agrees with reported data.[45, 46]

The N_2 adsorption desorption isotherm of Fe_3O_4-DA-Cu^+ and Fe_3O_4-DA-Ru^{2+} catalyst system and the corresponding pore-size distribution curve are shown in **Fig. 6 (a) and (b)**. A linear increase in the amount of adsorbed nitrogen was observed at a low relative pressure. This can be classified as a type of H_2 hysteresis loops. The catalyst Fe_3O_4-DA-Cu^+ exhibited IV-type curves (Fig 7(b)). For the For Fe_3O_4-DA-Cu^+ catalyst system, the BET surface area (S_{BET}), total pore volume (VP) and mean pore diameter (rp) for Fe_3O_4 was found to be respectively 45.31 m^2g^{-1}, 0.13 cm^3g^{-1}, and 2.1 nm respectively. For Fe_3O_4-DA-Ru^{2+} BET surface area (S_{BET}), total pore volume (VP) and mean pore diameter (rp) was found to be 85.33 m^2g^{-1}, 0.20 cm^3g^{-1}, and 4.8 nm respectively.
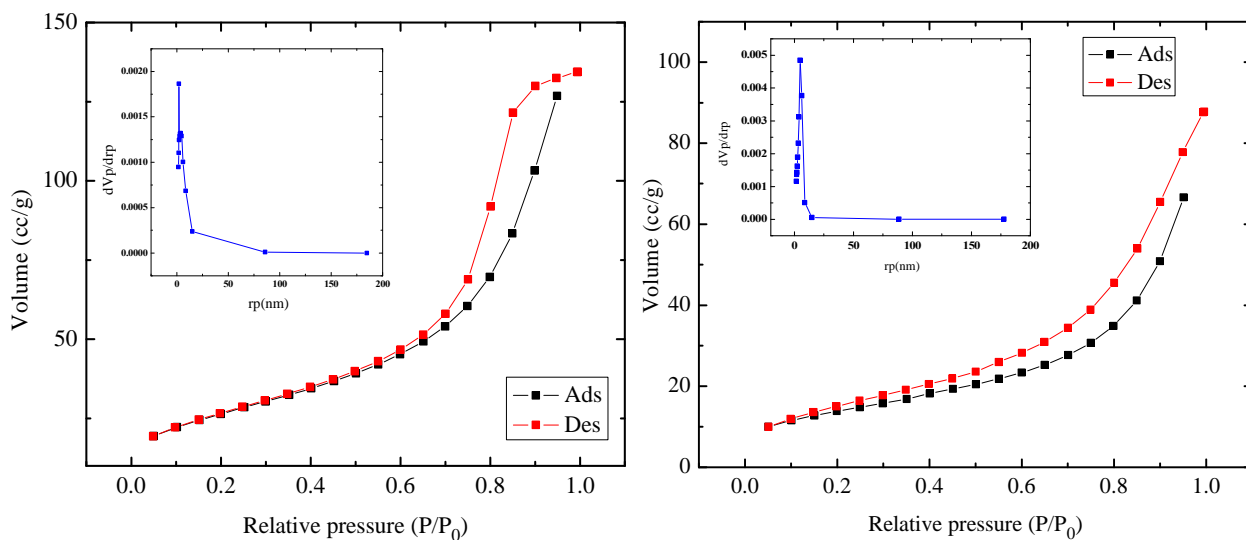
Fig. 6 N_2 adsorption–desorption isotherms of (a) Fe_3O_4@DA@Cu^+ and (b) Fe_3O_4@DA@Ru^{2+} nanocomposite catalytic system

The magnetic properties of the Fe_3O_4@DA@Cu^+ and Fe_3O_4@DA@Ru^{2+} catalytic systems were determined by a vibration sample magnetometer (VSM). The and magnetic hysteresis curves of both the systems are shown in **Fig. 7**. The magnetization Vs applied field curve for the catalyst system shows that the particles are superparamagnetic at room temperature.

The VSM curve for $Fe_3O_4@DA@Cu^+$ shows that its saturation magnetization value was 40 emu/g without the observation of hysteresis curves, indicating the typical superparamagnetic behaviour. The saturation magnetization of $Fe_3O_4@DA@Ru^{2+}$ is 30 emu/g that is large enough for the separation of the catalyst by applying an external magnetic field. This superparamagnetic behaviour for both Fe_3O_4 nanoparticles supported catalytic systems indicate the suitability of nanosized Fe_3O_4 as catalyst support for the magnetic separation.
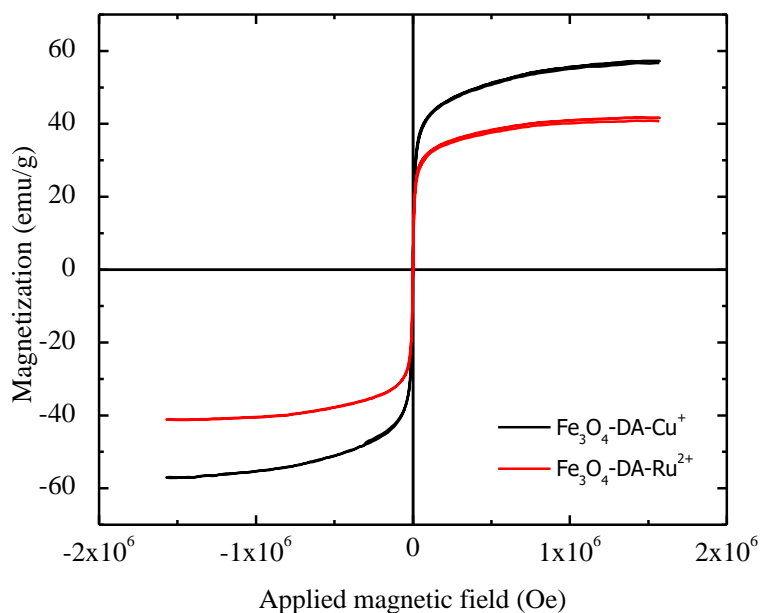
Fig. 7 Room-temperature magnetization curve of $Fe_3O_4@DA@Cu^+$ and $Fe_3O_4@DA@Ru^{2+}$ catalyst system

The amount of Cu in $Fe_3O_4@DA@Cu^+$catalyst was estimated from atomic absorption spectroscopy analysis and it was found to be 5 wt%. No significant loss in the Cu amount was found after five repeated reactions. Further, the concentration of Ru in $Fe_3O_4@DA@Ru^{2+}$ as estimated by atomic absorption spectroscopy analysis was 8.47 wt% before reaction. To monitor the changes in the composition of the catalyst, Ru ion concentration was estimated after 3 cycles

of reaction and found to be 6.31 %. This ~25 %loss of Ru is attributed to the leaching during the reflux condition and is an issue that needs to be addressed in future.

The photographic image of the catalyst system is shown in Fig. 8 (a). The Fe_3O_4-DA-M^{x+} catalyst is well dispersed 1-4 dioxane solvent. This better homogeneity of the catalyst in reaction medium enhances the reactivity when compared with conventional heterogeneous catalysts. After reaction the catalyst is easily separable from reaction medium by applying an external magnetic field Fig. 8 (b).
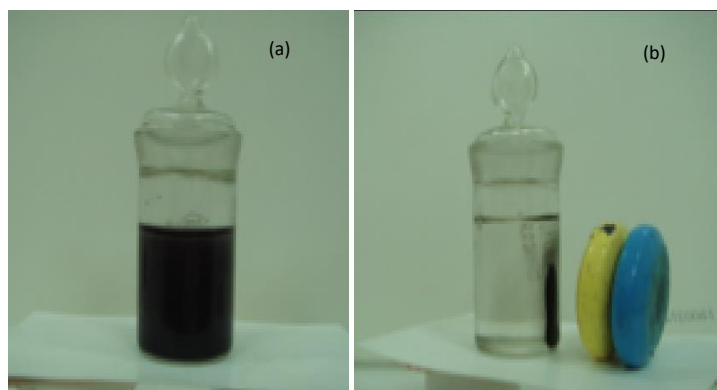

Fig. 8 Photographic image of (a) highly dispersed $Fe_3O_4@DA@Cu^+$ catalyst in 1-4 dioxane (b) catalyst separated under the influence of magnetic field.

Catalytic Performance of $Fe_3O_4@DA@Cu^+$ catalyst

The prepared magnetically recoverable and reusable catalyst was applied for carrying out the Cu-catalyzed azide–alkyne cycloaddition (CuAAC) reactions leading to the regioselective formation of 1,2,3-triazoles. Phenylacetylene and benzyl azide were chosen for the purpose of optimizing the reaction conditions for the cycloaddition (CuAAC) reactions. The optimization was started by changing the amount of the catalyst. As shown in Table 1, no product was formed

in the absence of the catalyst after 24 h of the reaction (entry 1). The best yield was obtained

with 20 mg of the catalyst (entry 3). With a further increase in the catalyst amount, the yield of

Table 1. Optimization of reaction condition of cycloaddition reactions

3 mmol   1 mmol
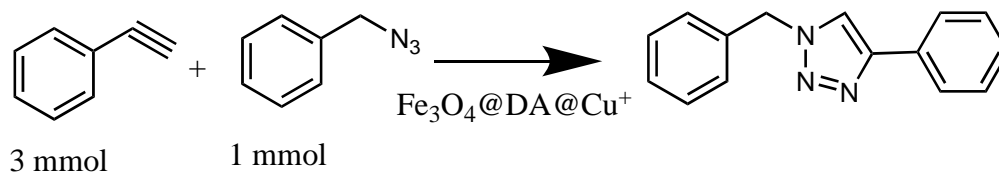
Entry	Amount of catalyst (mg)	Solvent	Temperature (°C)	Time (h)	Isolated Yield (%)
1	…….	1,4- dioxane	80	24	…….
2	40	1,4- dioxane	80	24	10
3	**20**	**1,4- dioxane**	**80**	**12**	**96**
4	40	1,4- dioxane	80	12	96
5	20	Water	80	12	55
6	20	Water: Ethanol (1:1)	80	24	55
7	20	Ethanol	80	24	55
8	10	1,4- dioxane	80	24	85
9	5	1,4- dioxane	80	24	75
10	20 (Fe_3O_4@DA)	1,4- dioxane	80	24	…….

the product was found to remain unchanged (entry 4). Among the various solvent systems

chosen to carry out the cycloaddition reaction, It was found that the most effective solvent

system for the cycloaddition reaction using our catalyst was 1,4-dioxane (entry 3). The

optimization table shows that the highest yield of 96 % was obtained with 20 mg of catalyst in 1-

4 dioxane for 12 h at 80 °C. It is also worth mentioning that no byproducts were observed under

the optimized conditions. The progress of the cycloaddition reactions was also tested using

dopamine modified Fe_3O_4 (without Cu) to confirm that the observed activity is only due to the Cu (I). The use of dopamine modified Fe_3O_4 (without Cu) showed no conversion after 24 h. This confirms that our catalyst system $Fe_3O_4@DA@Cu^+$ exhibits excellent catalytic activity for azide–alkyne cycloaddition.

The general applicability of the as prepared catalyst was also demonstrated in a variety of reactions of azide derivative with terminal alkyne derivatives (Table 2). The reaction between aliphatic/aromatic halides with acetylene derivatives in presence of sodium azide (Table 3) were also performed. In all the cases, the transformation reaction was completed with very good yields. Both aliphatic as well as aromatic azide and halides gave moderate to good yields of the corresponding triazole derivatives. The ^1H NMR spectra of all the isolated products are given in the SI Fig 3.

Catalytic Performance of $Fe_3O_4@DA@Ru^{2+}$ catalyst

The synthesized nanocomposite $Fe_3O_4@DA@Ru^{2+}$ was used a catalyst for transfer hydrogenation reaction of a series of aromatic ketones. In a typical reaction, 1 mmol of substrate was taken in 20 mL 0.1 M KOH in 2-propanol. KOH in 2-propanol serves as a reaction medium. The mixture was refluxed at 82°C for 18-24 h. Completion of the reaction was monitored by thin layer chromatography (TLC). Table 4 gives the summary of observations of transfer hydrogenation reaction of various aryl ketones over $Fe_3O_4@DA@Ru^{2+}$ catalyst. After completion of the reaction the catalyst was easily separated by an external magnet. Separated catalyst was then washed with acetone and dried in vacuum for further use. The ^1H NMR spectra of all the isolated products are given in the SI Fig 4.

Table 2: Cycloaddition of alkyl azide with terminal alkynes in the presence of $Fe_3O_4@DA@Cu^+$ catalyst
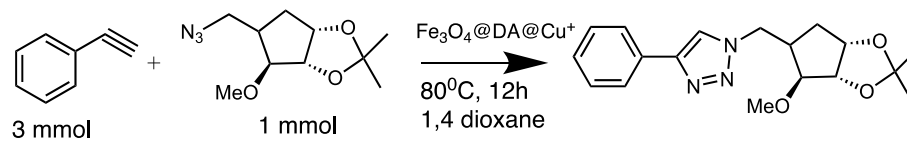
Entry	Azide derivatives	Acetylene derivatives	Major Product	Product Selectivity	Isolated Yield (%)
1				22:1	73.5
2				8:1	90
3				100	89
4				12:1	96
5				Not detected	70
6				Not detected	90

Table 3: Cycloaddition of alkyl halide with terminal alkynes in the presence of Sodium azide and Fe_3O_4@DA@Cu^+ catalyst.
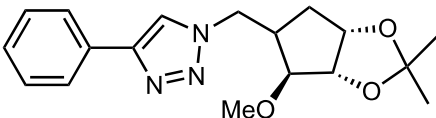

3 mmol	1 mmol	1.5 mmol	80^{0}C, 12h 1,4 dioxane	
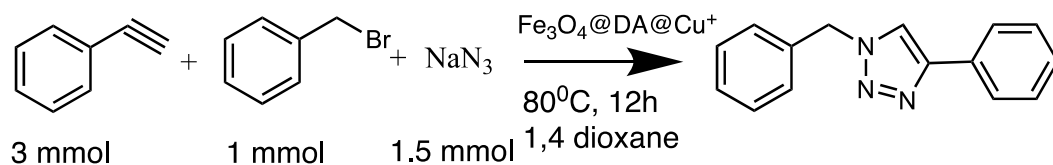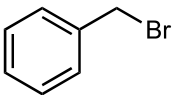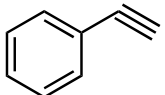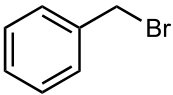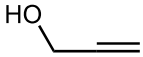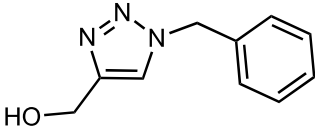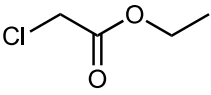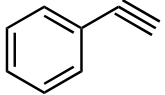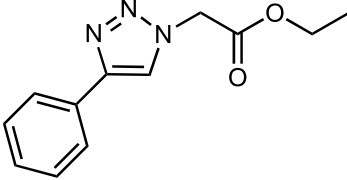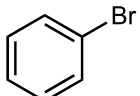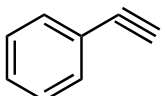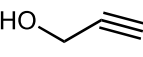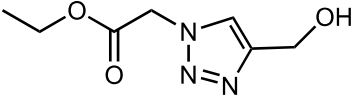
Entry	Halied derivatives	Acetylene derivatives	Major Product	Isolated Yield (%)
1				93
2				85
3				87
4			No reaction	......
5				70

Table 4: Cycloaddition of alkyl azide with terminal alkynes in the presence of Fe_3O_4@DA@Ru^{2+} catalyst

The reaction scheme at the top of the page:

Substrate: R-substituted acetophenone (aryl methyl ketone) with C=O

Conditions:
Fe$_3$O$_4$@DA@Ru^{2+}
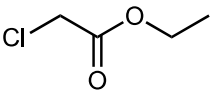1% KOH
in 2-propanol
Reflux

Product: R-substituted 1-arylethanol with OH
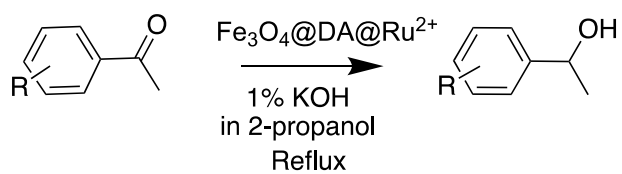
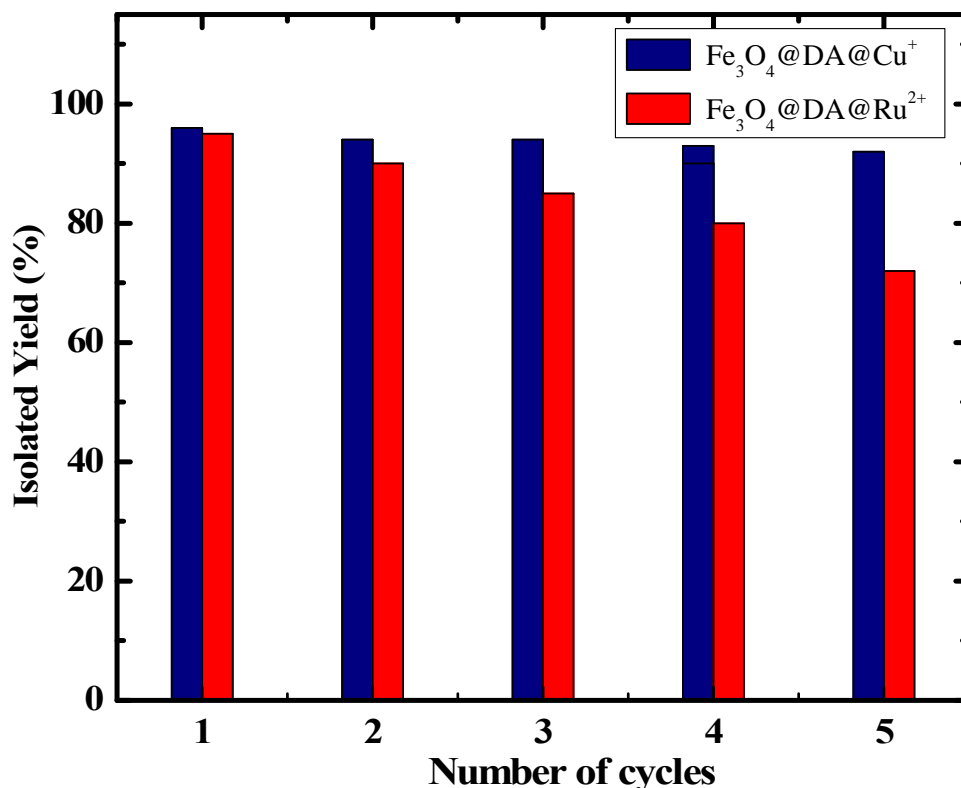| Entry	Substarte	Product	Time	Isolated Yield (%)
1	acetophenone	1-phenylethanol	18	92
2	4'-methoxyacetophenone	1-(4-methoxyphenyl)ethanol	18	86
3	2-acetylnaphthalene	1-(naphthalen-2-yl)ethanol	18	92
4	6-methoxy-2-acetylnaphthalene	1-(6-methoxynaphthalen-2-yl)ethanol	18	90
5	benzophenone	No reaction	36	0
6	4'-bromoacetophenone	1-(4-bromophenyl)ethanol	20	90
7	4'-iodoacetophenone	1-(4-iodophenyl)ethanol	18	92
8	4'-chloroacetophenone	1-(4-chlorophenyl)ethanol	18	91

Reusability test of Fe$_3$O$_4$@DA@M^{x+} catalyst system

Fig 9. Reusability of $Fe_3O_4@DA@M^{x+}$ catalyst system

The advantages of the application of heterogeneous catalyst system over its homogeneous counterpart is due to its easy separability, recyclability and reusability. Thus, it is extremely important to investigate these parameters. The reusability of $Fe_3O_4@DA@Cu^{1+}$ was tested in the synthesis of 1,4-substituted 1,2,3-triazoles by choosing the reaction between benzylbromide, phenylacetylene and sodium azide under the optimized reaction conditions. The catalyst was easily removed from the reaction mixture by the use of magnets and was washed with EtOH, and dried. The recovered catalyst showed no loss of activity up to the fifth run, after which the reaction started progressing slow due to the loss in its catalytic activity. When the rate of the reaction was extremely reduced, the catalyst was recovered from the reaction mixture was retreated. This regenerated catalyst exhibited the initial activity as a fresh catalyst. This demonstrates an extremely good regenerative capability for $Fe_3O_4@DA2Cu^+$ catalyst system

(Fig. 9). The reusability of $Fe_3O_4@DA@Ru^{2+}$ was investigated in the transfer hydrogenation reaction under optimized conditions. The loss in the activity of the catalyst after third run is due to the leaching of the catalyst, which is also in agreement with the AAS measurements discussed above.

Conclusions

In conclusion, we have developed a simple and effective superparamagnetic Fe3O4@Dopamine@Metal Ions (Metal Ions = Cu^+,Ru^{2+}) Nanocomposites as a heterogeneous catalytic systems by stabilizing copper and ruthenium ions on the surface-modified iron oxide nanoparticles. The synthesized $Fe_3O_4@DA@M^{x+}$ nanocatalysts have been used for the cycloaddition reaction of azides and alkynes and transfer hydrogenation reactions respectively. The use of an magnetic nanoparticle based heterogeneous catalyst is comparatively economical, experimentally simple, and, therefore, appealing for industrial use. The developed catalytic system is (a) reusable in up to five consecutive cycles without loss of catalytic activity and (b) easily recoverable by simply using an external magnet. The simplicity, efficiency and easy recoverability of the catalyst may lead to its applicability towards various scientific and industrial prospects.

Conflicts of interest

There are no conflicts to declare.

Acknowledgements

References

[1].   Arundhathi R, Damodara D, Likhar PR, Kantam ML, Saravanan P, Magdaleno T, Kwon SH (2011) Advanced Synthesis & Catalysis 353:1591-1600.

[2].   Stevens PD, Li G, Fan J, Yen M, Gao Y (2005) Chemical Communications 4435-4437.

[3].   Zhang Q, Su H, Luo J, Wei Y (2012) Green Chemistry 14:201-208.

[4].   Ranganath KV, Glorius F (2011) Catalysis Science & Technology 1:13-22.

[5].   Esmaeilpour M, Sardarian AR, Javidi J (2012) Applied Catalysis A: General 445:359-367.

[6].   Lu AH, Salabas EeL, Schüth F (2007) Angewandte Chemie International Edition 46:1222-1244.

[7].   Zhu Y, Stubbs LP, Ho F, Liu R, Ship CP, Maguire JA, Hosmane NS (2010) ChemCatChem 2:365-374.

[8].   Liu S, Yu B, Wang S, Shen Y, Cong H (2020) Advances in Colloid and Interface Science 102165.

[9].   Guin D, Baruwati B, Manorama SV (2007) Organic letters 9:1419-1421.

[10].   Baruwati B, Guin D, Manorama SV (2007) Organic Letters 9:5377-5380.

[11].   Du Q, Zhang W, Ma H, Zheng J, Zhou B, Li Y (2012) Tetrahedron 68:3577-3584.

[12].   De Cattelle A, Billen A, Brullot W, Verbiest T, Koeckelberghs G (2020) Macromolecules 53:1998-2005.

[13].   Zhang J, Fang Q, Duan J, Xu H, Xu H, Xuan S (2018) Langmuir 34:4298-4306.

[14].   Egorova KS, Ananikov VP (2016) Angewandte Chemie International Edition 55:12150-12162.

[15].   Wang W, Peng X, Wei F, Tung CH, Xu Z (2016) Angewandte Chemie International Edition 55:649-653.

[16].   Li S, Wang L, Yu F, Zhu Z, Shobaki D, Chen H, Wang M, Wang J, Qin G, Erasquin UJ (2017) Chemical science 8:2107-2114.

[17].   Moses JE, Moorhouse AD (2007) Chemical Society Reviews 36:1249-1262.

[18].   Kolb HC, Sharpless KB (2003) Drug discovery today 8:1128-1137.

[19].   Tornøe CW, Christensen C, Meldal M (2002) The Journal of Organic Chemistry 67:3057-3064.

[20].   Rostovtsev VV, Green LG, Fokin VV, Sharpless KB (2002) Angewandte Chemie International Edition 41:2596-2599.

[21].   Rodionov VO, Presolski SI, Gardinier S, Lim Y-H, Finn MG (2007) Journal of the American Chemical Society 129:12696-12704.

[22].   Chuprakov S, Kwok SW, Fokin VV (2013) Journal of the American Chemical Society 135:4652-4655.

[23].   Girard C, Önen E, Aufort M, Beauvière S, Samson E, Herscovici J (2006) Organic letters 8:1689-1692.

[24].   Chassaing S, Kumarraja M, Sani Souna Sido A, Pale P, Sommer J (2007) Organic letters 9:883-886.

[25].   Luong ND, Sinh LH, Johansson LS, Campell J, Seppälä J (2015) Chemistry–A European Journal 21:3183-3186.

[26].   Chung R, Vo A, Fokin VV, Hein JE (2018) ACS Catalysis 8:7889-7897.

[27].   Cernat A, Györfi SJ, Irimes M-B, Tertiş M, Bodoki A, Pralea I-E, Suciu M, Cristea C (2019) Electrochemistry Communications 98:23-27.

[28].   Tavassoli M, Landarani-Isfahani A, Moghadam M, Tangestaninejad S, Mirkhani V, Mohammadpoor-Baltork I (2016) ACS Sustainable Chemistry & Engineering 4:1454-1462.

[29].   Pourjavadi A, Motamedi A, Hosseini SH, Nazari M (2016) RSC Advances 6:19128-19135.

[30].   Wu W, Wang J, Wang Y, Huang Y, Tan Y, Weng Z (2017) Angewandte Chemie International Edition 56:10476-10480.

[31].   Xiong X, Cai L (2013) Catalysis Science & Technology 3:1301-1307.

[32].   Stanislaus A, Cooper BH (1994) Catalysis Reviews—Science and Engineering 36:75-123.

[33].   Widegren JA, Finke RG (2003) Journal of Molecular Catalysis A: Chemical 191:187-207.

[34].   Zang W, Li G, Wang L, Zhang X (2015) Catalysis Science & Technology 5:2532-2553.

[35].   Gilkey MJ, Xu B (2016) ACS catalysis 6:1420-1436.

[36].   Ikariya T, Blacker AJ (2007) Accounts of chemical research 40:1300-1308.

[37].   Morris RH (2009) Chemical Society Reviews 38:2282-2291.

[38].   Ito J-i, Nishiyama H (2014) Tetrahedron Letters 55:3133-3146.

[39].   Axet MR, Philippot K (2020) Chemical Reviews.

[40].   Kantam ML, Rao BPC, Choudary B, Sreedhar B (2006) Advanced synthesis & catalysis 348:1970-1976.

[41].   Gao J-X, Ikariya T, Noyori R (1996) Organometallics 15:1087-1089.

[42].   Buijsman RC, van Vuuren E, Sterrenburg JG (2001) Organic letters 3:3785-3787.

[43].   Dey TK, Ghosh K, Basu P, Molla RA, Islam SM (2018) New Journal of Chemistry 42:9168-9176.

[44].   Pachupate NJ, Vaidya PD (2018) Journal of environmental chemical engineering 6:883-889.

[45].   Rizescu C, Podolean I, Cojocaru B, Parvulescu VI, Coman SM, Albero J, Garcia H (2017) ChemCatChem 9:3314-3321.

[46].   Kaga Y, Abe Y, Yanagisawa H, Kawamura M, Sasaki K (1999) Surface Science Spectra 6:68-74.